

Topological effects of charge density waves in ring-shaped crystals of NbSe₃

Toru Matsuura,¹ Taku Tsuneta,² Katsuhiko Inagaki,¹ and Satoshi Tanda¹

¹*Department of Applied Physics, Hokkaido University, Kita-ku, Sapporo 060-8628, Japan*

²*Low Temperature Laboratory, Helsinki University of Technology, Otakaari 3A, Espoo, Finland*

(Received 29 November 2005; revised manuscript received 10 March 2006; published 19 April 2006)

We studied the differences of the charge density wave (CDW) dynamics in closed-ring and open-ring topologies by measuring the frequency-dependent resistance in the radio-frequency range. We performed a two-probe ac resistance measurement for a ring-shaped crystal of niobium triselenide (NbSe₃) in the 300 kHz to 1.3 GHz frequency range. We compared the frequency dependence of the resistance of closed-ring and open-ring crystals and found that the pinning potential in the former is smaller than that in the latter. The open-ring crystal was obtained by changing of the topology of the closed-ring crystal. We believe that the reduction in the pinning effect is caused by a CDW circulating current in the closed-ring topology.

DOI: [10.1103/PhysRevB.73.165118](https://doi.org/10.1103/PhysRevB.73.165118)

PACS number(s): 71.45.Lr, 02.40.-k

I. INTRODUCTION

Nontrivial real-space topology plays an important role in physical systems.^{1,2} Topology deals with invariant properties in continuous transformation. For example, a ring is a fundamental topological structure, because the hole in the ring cannot be eliminated by continuous transformation. The physical systems with a ring topology should exhibit topological effects, such as the Aharonov-Bohm (AB) effect,³ due to the nontrivial real-space topology. It is possible to change physical properties by changing the real-space topology.

A charge density wave (CDW) is the best system with which to investigate the effects of real-space topology, because of the interaction between a CDW and a real space, in this case a crystal, through electron-phonon coupling. The CDW-ordered state is a macroscopic quantum state resulting from real-space ordering.⁴ A CDW has rich electrical properties such as the nonlinear current-voltage (I - V) characteristic,⁵ narrow-band noise,⁶ and frequency-dependent resistance.^{7,8} The CDW was proposed as a model of superconductivity by Fröhlich in 1954, because an incommensurate CDW can flow without dissipation in an ideal crystal.⁹ In reality, a CDW supercurrent has never been observed because the crystal edges or impurities act as pinning centers. If the edges of a CDW system could be connected, it would become an edgeless CDW ring. The supercurrent would then exist in the ring as a result of the change in topology. Moreover, the CDW ring has been expected to exhibit topological effects associated with Berry's phase.¹⁰⁻¹³ The pioneering experimental study of the AB effect in the CDW system was undertaken by Latyshev *et al.*¹⁴ They measured a quasi-one-dimensional conductor with many columnar defects since no one could make a CDW ring. We need a CDW ring to enable us to study the topological effects in CDW's.

The Hokkaido group succeeded in synthesizing exotic topological crystals of NbSe₃, which form rings, Möbius strips (π twisted rings), and figure-eight loops (2π twisted rings) with diameters of 10–200 μm .^{1,15,16} NbSe₃ is a typical CDW material that shows two metal-incommensurate CDW transitions at $T_{C1}=144$ K and $T_{C2}=59$ K,¹⁷ and CDW transitions

have also been observed in topological crystals.^{15,16} They have provided new experimental systems for investigating the effects of topology on the CDW properties. Since the CDW phase-phase correlation length ξ_{CDW} is comparable to the circumference of the CDW ring, the topological crystals are one-dimensional closed rings. The nontrivial topologies of their forms have been expected to change the CDW properties. Some topological effects have already been observed in the electrical properties including an anomaly in the nonlinear I - V characteristic in a NbSe₃ ring¹⁸ and a reduction in the transition temperatures in rings and figure-eight loops.¹⁹

Here we report a difference between the CDW dynamics of two topologies: namely, a closed-ring topology and an open-ring topology. We measured the frequency-dependent resistance of a ring crystal of NbSe₃ to investigate the CDW dynamics. First, we measured a ring crystal with the closed-ring topology. Then, we measured a crystal with the open-ring topology, which we obtained by performing topology-change surgery on the ring crystal. The closed-ring topology of a ring crystal can be surgically changed to an open-ring topology by using a focused ion beam (FIB), as shown in Fig. 1.²⁰ An open ring is topologically different from a closed ring because it has two edges. Using this method, we can study two CDW's, which are identical except for their topology, and avoid the sample dependence.²¹ The frequency-dependent resistance measurement was performed in the 300 kHz to 1.3 GHz range below the first CDW transition temperature T_{C1} . We found that the pinning potential of the CDW in the closed-ring topology was smaller than that in the open-ring topology. The reduction of the pinning effect in the closed-ring topology suggests that the circulating current mode plays an important role. This effect was revealed by the topology-change surgery.

II. EXPERIMENT

The ring crystals of NbSe₃ are synthesized by a chemical vapor transportation method. Nb and Se powders with a 1:3 molar ratio are enclosed in an evacuated quartz tube and soaked at 740 °C for a few hours using a furnace with an appropriate temperature gradient. The crystals acquire their

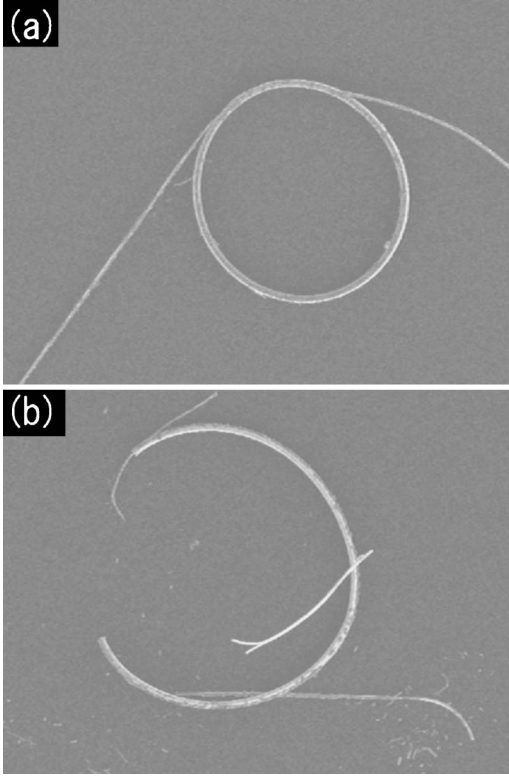


FIG. 1. (a) Scanning ion beam microscopy (SIM) image of a typical ring crystal with a radius of $18.2 \mu\text{m}$ and a thickness of $0.47 \mu\text{m}$. It is a closed ring. (b) SIM image of the ring crystal after focused ion beam (FIB) surgery. The FIB surgery provided two edges in the ring crystal. The forms in (a) and (b) are referred to in the text as a closed-ring topology and an open-ring topology, respectively. This is a useful method for investigating topology dependence alone, without sample dependence.

topological forms by a previously reported mechanism.¹

We performed a two-probe ac resistance measurement for a ring-shaped crystal of NbSe_3 in the closed-ring and open-ring topologies. The ac resistance measurement is a useful way to investigate the CDW dynamics in topological crystals because it does not require a current injection via contacts. Current injection causes a phase slip near the contacts,²² and this acts as a pinning center.²³ The current injection may change the topological property of the CDW ring. On the other hand, frequency-dependent resistance measurement does not require the current injection. The CDW dynamics is expressed by the damped oscillation.^{7,8} The single-coordinate model is

$$\frac{d^2\phi}{dt^2} + \Gamma \frac{d\phi}{dt} + \omega_0^2 \sin \phi = -\frac{n\pi e}{m^*} E(t), \quad (1)$$

where ϕ is the CDW phase, Γ is the damping constant, and ω_0^2 is the pinning potential. The right-hand side indicates an external force. The CDW current is expressed as

$$I_{\text{CDW}} = -\frac{e}{\pi} \frac{d\phi}{dt}. \quad (2)$$

The CDW contributes electrical conduction as a displacement current in the ac electric field. When the applied volt-

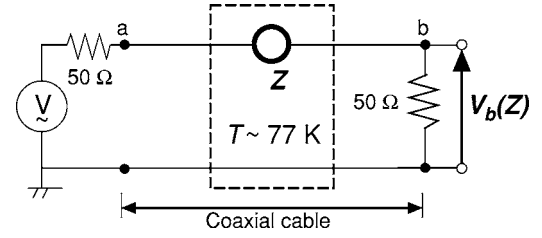


FIG. 2. Electrical circuit for the frequency-dependent resistance measurement. The ring at the center of the circuit indicates a ring crystal, which is attached to two contacts.

age is small and the frequency f is much smaller than $\omega_0/2\pi$, conductivity is expressed by the Drude law

$$\sigma_{\text{CDW}}(\omega) = \sigma_{\infty} \frac{i\omega/\omega_C}{1 + i\omega/\omega_C}. \quad (3)$$

Here we neglect the inertial term $d^2\phi/dt^2$ and assume $\sin \phi \approx \phi$ and we use the characteristic frequency $\omega_C = \omega_0^2/\Gamma$. The CDW dynamical parameters can be investigated by measuring the frequency-dependent resistance. While the measurement voltage remains smaller than the threshold voltage of a CDW sliding state, we can avoid the effect of current injection. Therefore, the frequency-dependent resistance measurement is advantageous in terms of investigating the CDW in the topological crystals.

The frequency-dependent resistance was measured as follows. A NbSe_3 ring crystal, with a diameter of $40 \mu\text{m}$ and a width and thickness both less than $1 \mu\text{m}$, was fixed on a sapphire insulator plate. We attached two contacts to the sample to enable to supply an ac voltage. The plate was placed on a Cu block in the vacuum chamber of a cryostat. The crystal was cooled to 77 K by liquid nitrogen, and we measured the temperature dependence of the resistance while heating the crystal from 77 K to room temperature. We used the conventional transmission method for the frequency-dependent resistance measurement with a Hewlett-Packard HP8712ET network analyzer in a frequency range of $f = 300 \text{ kHz}$ to 1.3 GHz. The measurement circuit is shown in Fig. 2. The voltage amplitude was kept below the threshold voltage of the sample. The sample impedance Z is measured by using the following equation:

$$Z = Z_0 \frac{1/V - 1/V_s}{1/V_0 - 1/V_s}, \quad (4)$$

where $\omega = 2\pi f$, Z_0 is a standard impedance, and $\mathbf{V} = \mathbf{V}_b(\mathbf{Z}(\omega, T)) = |\mathbf{V}|e^{i\phi}$ is the complex voltage at b in Fig. 2, which is a function of the sample impedance $\mathbf{Z}(\omega, T) = R(\omega, T) + iX(\omega, T)$. Other parameters $\mathbf{V}_s = \mathbf{V}_b(0)$ and $\mathbf{V}_0 = \mathbf{V}_b(Z_0)$ are used to calibrate the frequency dependence of the finite loss and phase delay in the cables. Since the calibration parameters depended on the temperature sweep, we calibrated both frequency and temperature. After measuring the frequency-dependent resistance of the closed-ring topology, we performed FIB surgery on the ring crystal to change to be the open-ring topology. We then again measured the frequency-dependent resistance of the pinning state and compared the results we obtained for the two topologies.

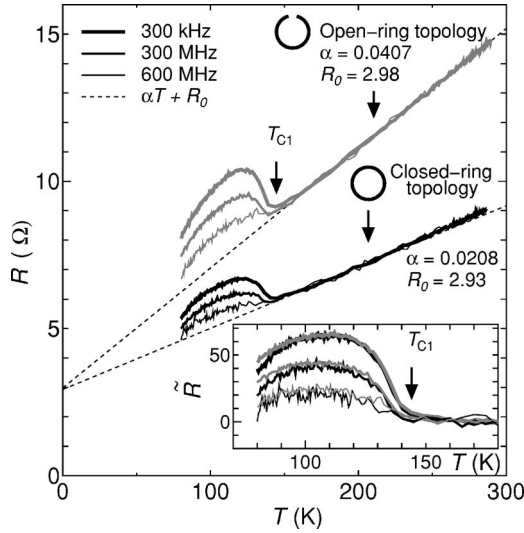


FIG. 3. Temperature dependence of resistance in a closed-ring topology and in an open-ring topology. The line thickness indicates the frequencies, and the dashed lines are linear fitting lines, $R(T) = \alpha T + R_0$, fitted to the metallic region in the 160–200-K range. The inset shows the temperature dependence of the normalized resistance, $\tilde{R}(\omega, T) = [R(\omega, T) - R_0] / \alpha - T$. The first CDW transition temperature T_{C1} is ~ 145 K in both topologies. The resistance peak below T_{C1} is maximum at the same temperature.

III. RESULTS AND DISCUSSIONS

We observed a CDW transition with a resistance increase at ~ 145 K in both topologies. Figure 3 shows the temperature dependence of the resistance $R(\omega, T)$ [real part of impedance $\mathbf{Z}(\omega, T)$] in the closed-ring and open-ring topologies in the 77-K-to-room-temperature range, at frequencies of 300 kHz, 300 MHz, and 600 MHz. The sample is metallic above 150 K because the resistance in each topology is proportional to temperature. Below the CDW transition temperature, the resistance increases because the electron density decreases as a result of the metal-CDW transition. The resistance shows a peak at 120 K and decreases proportionally below 100 K, because uncondensed electrons remain even below T_{C1} in NbSe₃. The second transition was not observed in this measurement because T_{C2} was below 77 K.

In the CDW state R decreases with increases in frequency. This behavior is explained by the CDW collective displacement around the pinning center with a finite damping time and corresponds to the results of a previous experiment for NbSe₃ whiskers.^{7,8} There is almost no frequency dependence in the low-frequency region below 1 MHz. Therefore, we assumed the temperature dependence at 300 kHz to be the same as that at a dc voltage. The dashed lines seen in Fig. 3 are fitting lines for $R_{\text{fit}}(T) = \alpha T + R_0$ at 300 kHz, where T is the temperature. We fit lines in the 160–200-K range for both sets of data. This is just above the transition temperature. The temperature coefficient α is 0.0208 in the closed-ring topology and 0.0407 in the open-ring topology. α doubled as a result of the topology change. This corresponds to one of the two current paths being eliminated by the FIB surgery. On the other hand, the intercept R_0 is 2.93 Ω in the

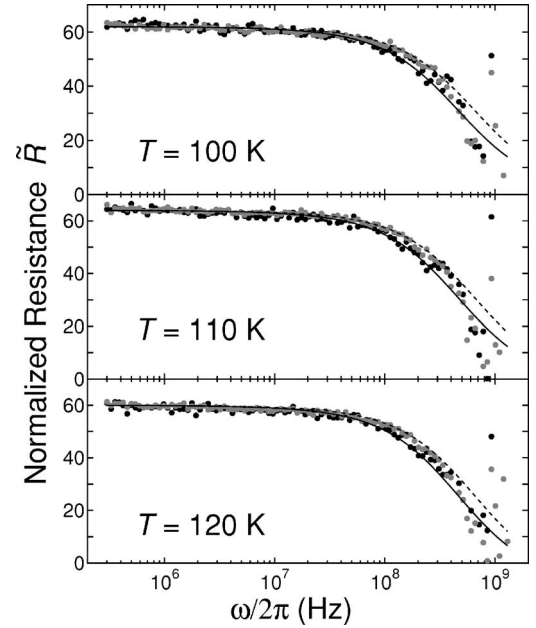


FIG. 4. The frequency dependence of the normalized resistance, $\tilde{R}(\omega, T) = [R(\omega, T) - R_0] / \alpha - T$, at $T = 100, 110,$ and 120 K below the first CDW transition temperature $T_{C1} = 145$ K. The black dots are experimental data for the closed-ring topology, and the gray dots are data for the open-ring topology. The solid and dashed lines indicate the fitting curves given in the text for the closed-ring and open-ring topologies, respectively. The fitting parameter β is set at 0.8 in both topologies and for all temperatures. The characteristic frequency $\omega_C / 2\pi$ is 0.85 GHz in the closed-ring topology and 1.2 GHz in the open-ring topology at all temperatures.

closed-ring topology and 2.98 Ω in the open-ring topology. R_0 does not depend on the topology change and so must represent the contact resistances. These results are consistent with the elimination of one path by topology-change surgery. Therefore, we considered that the surgery was successful. We then normalized the resistance using α and R_0 to compare the frequency dependences. We disregard the temperature dependence of R_0 because it is sufficiently smaller than that of the sample. Thus, we can define the normalized resistance $\tilde{R}(\omega, T) = [R(\omega, T) - R_0] / \alpha - T$. The inset shows \tilde{R} as a function of temperature T . The temperature dependence of \tilde{R} at 300 kHz corresponds in both topologies. However, it does not correspond at high frequencies.

We found that the frequency dependence of the normalized resistance \tilde{R} is different for the two topologies. Figure 4 shows the frequency dependence of \tilde{R} at 100, 110, and 120 K. The black dots are experimental data for the closed-ring topology, and the gray dots are data for the open-ring topology. Each \tilde{R} value decreases with an increase of frequency above 100 MHz. We found that the frequency dependence was changed by changing the topology. The resistance of the closed-ring topology starts to decrease at a lower frequency than that of the open-ring topology. We fitted the results using the following empirical curve, which was used for NbSe₃ by Wu *et al.*:²⁴

$$\sigma_{\text{CDW}}(\omega) = \sigma_{\infty} \frac{(i\omega/\omega_C)^{\beta}}{1 + (i\omega/\omega_C)^{\beta}}. \quad (5)$$

This expression is Eq. (2) modified by the empirical parameter β , which represents the random distribution of weak pinning centers by the impurities.²⁴ We assumed that the total conduction is the sum of that of the CDW and quasiparticles. Hence,

$$\sigma_{\text{total}}(\omega) = \sigma_{\text{metal}} + \sigma_{\text{CDW}}(\omega) \quad (6)$$

and

$$R(\omega) \propto \text{Re}[\sigma_{\text{total}}^{-1}(\omega)]. \quad (7)$$

The solid and dashed curves in Fig. 4 indicate the fitted curves for the closed-ring and open-ring topologies, respectively. We set $\tilde{R}(\omega=0)=62, 64,$ and 60 at $T=100, 110,$ and 120 K, respectively. When the system follows the single-coordinate model, $\beta=1$. In reality, the random distribution of weak pinning centers modulates the CDW phase locally. In our sample, $\beta=0.8$ in both topologies and at $100, 110,$ and 120 K. The distributions of the pinning centers in both paths are the same. These parameters have the same values in both topologies, except for the characteristic frequency $\omega_C/2\pi$. We found that the characteristic frequency was changed by the surgery. $\omega_C/2\pi=0.85$ GHz in the closed-ring topology and 1.2 GHz in the open-ring topology at all three temperatures. ω_C became about 1.4 times larger as a result of the topology change. $\omega_C=\omega_0^2/\Gamma$, where Γ is the damping constant of the CDW, and ω_0^2 is the pinning potential. Since Γ is proportional to σ_{∞}^{-1} , which was unchanged by the surgery, this result suggests that the pinning potential in the closed-ring topology is greatly suppressed.

Why does the topology of the crystal affect the pinning? The result cannot be explained by the simplest parallel circuit model. When we assume that a closed-ring topology corresponds to a parallel circuit of two CDW materials, the pinning potential is unchanged by the surgery, because the normalized resistance does not depend on the number of paths. It is possible that the strain energy of the crystal was changed by the change of topology.²⁵ However, the strain energy of the remaining path was not changed by the surgery because the sample was fixed at two points on a sapphire plate by silver paste. We therefore considered the effect of the edges or the interaction between the two current paths.

Next, we discuss the elastic energy of the CDW phase, which must differ depending on the topology. In the open-ring topology, the edges act as strong pinning centers. In an electric field, the CDW is compressed near one edge and expanded near the other edge. The elastic energy increases the pinning potential energy. On the other hand, there are two CDW current paths in the closed-ring topology. Therefore, the CDW is compressed and expanded near the contacts under the ac electric field in an ac closed-ring topology. The increases in the pinning potential in the closed-ring topology must be larger than those for the open-ring topology because of the existence of the two current paths. This is inconsistent with the experimental result and suggests that we need another explanation.

A possible explanation is that a circulating current in the ring affects the pinning. The Fröhlich supercurrent can flow in an impurity-free ring crystal without dissipation because of the absence of edges.⁹ We believe that the CDW circulating current mode is excited by the ac electric field in the closed-ring topology. The phase-phase correlation length is greater than the average impurity length. Impurities act as weak pinning centers that modulate phase locally. Therefore, it is reasonable to consider that the CDW correlation length exceeds the circumference of the ring crystal. Nevertheless, the circulating current mode certainly does not exist in the open-ring topology. We believe that the circulating current mode is the key to the decrease in the pinning potential in the closed-ring topology.

IV. CONCLUSION

We found that the pinning potential of a CDW in a closed-ring topology was smaller than that in an open-ring topology by measuring ac resistance of a NbSe₃ ring crystal. The difference is caused by the circulating current mode in the closed-ring topology.

ACKNOWLEDGMENTS

The authors are grateful to K. Yamaya, T. Toshima, and K. Shimatake for stimulating discussions. This research was supported by the 21 COE program on Topological Science and Technology from the Ministry of Education, Culture, Sport, Science and Technology of Japan and the Japan Society for the Promotion of Science.

¹S. Tanda, T. Tsuneta, Y. Okajima, K. Inagaki, K. Yamaya, and N. Hatakenaka, *Nature (London)* **417**, 397 (2002).

²C. Nash and S. Sen, *Topology and Geometry for Physics* (Academic Press, New York, 1983).

³Y. Aharonov and D. Bohm, *Phys. Rev.* **115**, 485 (1959).

⁴G. Grüner, *Rev. Mod. Phys.* **60**, 1129 (1988).

⁵P. Monceau, N. P. Ong, A. M. Portis, A. Meerschaut, and J. Rouxel, *Phys. Rev. Lett.* **37**, 602 (1976).

⁶R. M. Fleming and C. C. Grimes, *Phys. Rev. Lett.* **42**, 1423 (1979).

⁷G. Grüner, L. C. Tippie, J. Sanny, W. G. Clark, and N. P. Ong, *Phys. Rev. Lett.* **45**, 935 (1980).

⁸D. Reagor, S. Sridhar, and G. Grüner, *Phys. Rev. B* **34**, 2212 (1986).

⁹H. Fröhlich, *Proc. R. Soc. London, Ser. A* **232**, 296 (1954).

¹⁰M. V. Berry, *Proc. R. Soc. London, Ser. A* **392**, 45 (1984).

¹¹E. N. Bogachek, I. V. Krive, I. O. Kulik, and A. S. Rozhavsky, *Phys. Rev. B* **42**, 7614 (1990).

¹²Ya-Sha Yi and A. R. Bishop, *Phys. Rev. B* **58**, 4077 (1998).

¹³G. Montambaux, *Eur. Phys. J. B* **1**, 377–383 (1998).

- ¹⁴Yu. I. Latyshev, O. Laborde, P. Monceau, and S. Klaumünzer, *Phys. Rev. Lett.* **78**, 919 (1997).
- ¹⁵S. Tanda, H. Kawamoto, M. Shiobara, Y. Sakai, S. Yasuzuka, Y. Okajima, and K. Yamaya, *Physica B* **284**, 1657 (2000).
- ¹⁶T. Tsuneta and S. Tanda, *J. Cryst. Growth* **264**, 223 (2004).
- ¹⁷J. Chaussy, P. Haen, J. C. Lasjaunias, P. Monceau, G. Waysand, A. Waintal, A. Meerschaut, P. Molinié, and J. Rouxel, *Solid State Commun.* **20**, 759 (1976).
- ¹⁸Y. Okajima, H. Kawamoto, M. Shiobara, K. Matsuda, S. Tanda, *Physica B* **284**, 1659 (2000).
- ¹⁹T. Tsuneta, S. Tanda, K. Inagaki, Y. Okajima, and K. Yamaya, *Physica B* **329–333**, 1544 (2003).
- ²⁰T. Matsuura, S. Tanda, K. Asada, Y. Sakai, T. Tsuneta, K. Inagaki, and K. Yamaya, *Physica B* **329**, 1550 (2003).
- ²¹J. McCarten, D. A. DiCarlo, M. P. Maher, T. L. Adelman, and R. E. Thorne, *Phys. Rev. B* **46**, 4456 (1992).
- ²²S. G. Lemay, M. C. de Lind van Wijngaarden, T. L. Adelman, and R. E. Thorne, *Phys. Rev. B* **57**, 12781 (1998).
- ²³M. Prester, *Phys. Rev. B* **32**, 2621 (1985).
- ²⁴Wei-yu Wu, L. Mihály, George Mozurkewich, and G. Grüner, *Phys. Rev. B* **33**, 2444 (1986).
- ²⁵Jahyoug Kuh, Y. T. Tseng, Kwith Wagner, Jay Brooks, G. X. Tessema, and M. J. Skove, *Phys. Rev. B* **57**, 14576 (1998).